Communication

Formation of Trioctylamine from Octylamine On Au(111)

Sigrid Weigelt, Joachim Schnadt, Anders K. Tuxen, Federico Masini, Christian Bombis, Carsten Busse, Cristina Isvoranu, Evren Ataman, Erik Lægsgaard, Flemming Besenbacher, and Trolle R. Linderoth

J. Am. Chem. Soc., **2008**, 130 (16), 5388-5389 • DOI: 10.1021/ja710227g • Publication Date (Web): 02 April 2008

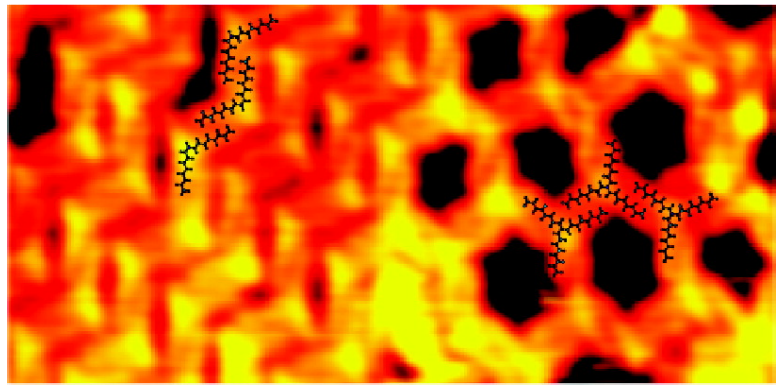

J|A|C|S
COMMUNICATIONS

Published on Web 04/02/2008

Formation of Trioctylamine from Octylamine On Au(111)

Sigrid Weigelt,[†] Joachim Schnadt,[‡] Anders K. Tuxen,[†] Federico Masini,[†] Christian Bombis,[†] Carsten Busse,[†] Cristina Isvoranu,[‡] Evren Ataman,[‡] Erik Lægsgaard,[†] Flemming Besenbacher,[†] and Trolle R. Linderoth*[,†]

Interdisciplinary Nanoscience Center (iNANO) and Department of Physics and Astronomy, University of Aarhus, Building 1520, Ny Munkegade, 8000 Aarhus C, Denmark, and Department of Synchrotron Radiation Research, Lund University, Box 118, 221 00 Lund, Sweden

Received November 21, 2007; E-mail: trolle@inano.dk

The adsorption of aliphatic amines on transition metal surfaces has been studied extensively, motivated mainly by amine-related heterogeneous catalysis[1] and the potential use of alkylamines as corrosion inhibitors.[2] The studies have focused primarily on the decomposition of methylamine caused by thermal treatment, and it has been shown that the fragmentation route is substrate-dependent.[3–8] At the Cu(211) surface, the presence of oxygen results in dehydrogenation and further reactions cause formation of dimethylamine.[3] On Cr(100) and Cr(111), methylamine undergoes C−N bond cleavage.[9] Investigations of other aliphatic amines exist, such as decylamine on a Au/Si[10] surface, dimethylamine and ethylamine on Cu(211),[1] and trimethylamine on Pt(111).[11] Common to all these studies is that they have been obtained with surface averaging techniques. In contrast, scanning probe investigations, which provide spatial information on the amine layers, are very scarce and have mainly been performed on semiconductor surfaces.[12–14]

Here, we investigate the adsorption of octylamine on Au(111) motivated by related studies of surface reactions and self-assembly.[15] We surprisingly find that octylamine undergoes a thermally activated chemical reaction, resulting in formation of trioctylamine as confirmed both by X-ray photoelectron spectroscopy (XPS) and by comparison to the scanning tunneling microscopy (STM) signature of trioctylamine deposited directly onto the Au(111) surface (for structures of the compounds, see Figure S1).

The STM experiments were performed in an ultrahigh vacuum system equipped with the home-built Aarhus STM.[16] XPS results were obtained at beam line I311 at MAX laboratory.[17] The herringbone reconstructed Au(111)-(22 × $\sqrt{3}$) surface was prepared by argon-ion sputtering at 1.5 kV followed by annealing to 850 K. Octylamine (99%, Sigma-Aldrich) and trioctylamine (99.9%, Sigma-Aldrich) were loaded in glass vials and dosed through a leak valve. All STM images were recorded at temperatures between 110 and 150 K.

Octylamine was deposited at a pressure of 1–2 × 10^{-8} mbar for 1 min onto the Au(111) surface held at room temperature. This resulted in a self-assembled lamellar structure[15] (Figure 1a,b) in which the alkyl chains are arranged parallel with the surface and stacked into rows (lamellae) running along a <1 1 –2> high symmetry direction with a preference for molecular stacking along the ridges of the herringbone reconstruction (see also Figure S2). All molecules within a row have their axis rotated by an angle of ±(11 ± 1)° with respect to a <1 –1 0> high symmetry direction. The sense of rotation alternates between adjacent rows. The rectangular unit cell contains two molecules and has dimensions $a = 5.2 \pm 0.4$ Å and $b = 26.3 \pm 1$ Å as depicted in Figure 1b.

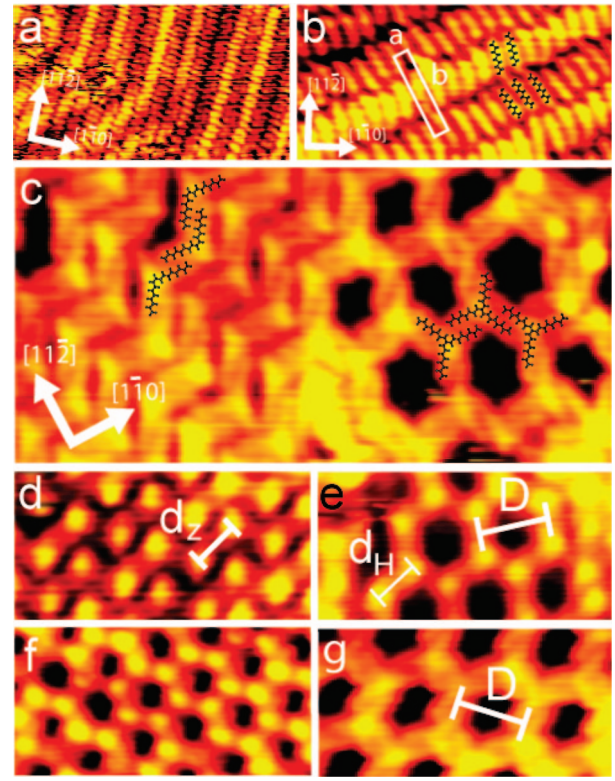

Figure 1. STM images of amines on Au(111). (a) Large-scale ($I_t = 0.46$ nA, $V_t = 1.8$ V, image size 216 × 150 Å^2) and (b) high-resolution ($I_t = 0.41$ nA, $V_t = 2.0$ V, image size 100 × 50 Å^2) image of the lamellar adsorption structure formed after deposition of octylamine at room temperature. (c−e) Structures observed upon annealing to 400 K as observed in two different imaging modes, revealing either (c) the molecular backbones ($I_t = 0.44$ nA, $V_t = 2.0$ V, image size 170 × 85 Å^2) or (d,e) the nitrogen atoms ($I_t = 0.35/0.34$ nA, $V_t = 2.0/1.7$ for d/e, image sizes 100 × 50 Å^2). Two structures are found with zigzag (d) or a honeycomb pattern (e). (f,g) Honeycomb structure formed by trioctylamine observed in both (f) the nitrogen imaging mode ($I_t = 0.37$ nA, $V_t = 2.1$ V, image size 150 × 75 Å^2) and (g) the backbone imaging mode ($I_t = 0.38$ nA, $V_t = 2.0$ V, image size 100 × 50 Å^2).

Upon thermal annealing to ∼400 K, the molecular layer undergoes an irreversible structural change (see Figure 1c−e), resulting in two coexisting phases, an open honeycomb structure (right side) and dense zigzag rows (left side). The image in Figure 1c is obtained in an STM tip imaging mode, revealing the individual alkyl chains, whereas the images in Figures 1d,e are dominated by bright protrusions attributed to moieties comprising one or more N atoms.

[†] University of Aarhus.
[‡] Lund University.

10.1021/ja710227g CCC: $40.75

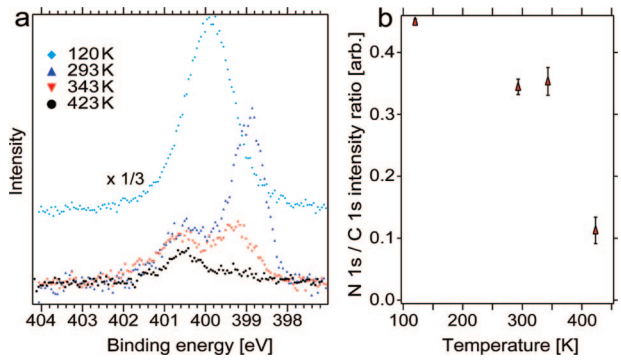

Figure 2. XPS results for octylamine on Au(111) (a) N 1s spectra, obtained after annealing to the temperatures indicated (all spectra acquired at ~120 K). (b) Plot of the relative N 1s/C 1s intensity as a function of annealing temperature.

The alkyl chains in the structures are oriented along <1 –1 0> directions. The honeycomb structure can be rationalized as trimeric units formed from three alkyl chains joined in a common node and separated by 120° angles. Six such trimers can be joined pairwise tail-along-tail as depicted in Figure 1c, resulting in a hexagonal pore of $D = 27 \pm 2$ Å diameter. In the zigzag rows, only two alkyl chains, forming a dimer, meet head-to-head in a 120° angle. The dimers are joined tail-to-tail as seen in Figure 1c. The distance $d_z = 15 \pm 2$ Å ($d_H = 15 \pm 2$ Å) (Figure 1d,e) between two head-to-head meeting points in the zigzag phase (honeycomb phase) are identical. The structures are still found upon annealing to 500 K, considerably above the desorption temperature ($T < 280$ K) of alkanes with similar chain length.[18]

In contrast to the lamellar structure, the new phases could only be observed at positive sample bias. At negative bias, the underlying herringbone-reconstructed Au(111) substrate is imaged instead (Figure S3). This indicates that the irreversible structural transformation is accompanied by a change in the energies of the molecular orbitals signaling a chemical change.

To obtain information about the chemical state of the adsorbed molecules, we performed X-ray photoelectron spectroscopy. For the XPS measurements, octylamine was dosed at a pressure of 10^{-7} mbar for 6 min onto a sample held below 120 K. The N 1s XPS spectra are shown in Figure 2a. The multilayer spectrum obtained below 120 K displays a single peak with a binding energy of 399.8 eV. A shift to 398.9 eV along with the appearance of an additional minor high-energy peak at 400.4 eV is observed upon annealing to 293 K. Further annealing to 343 K results in a narrowing of the main peak associated with an upward energy shift to 399.2 eV and a possible slight change of the high-energy peak to 400.6 eV. As the surface temperature reaches 423 K, the low-energy peak at 399.2 eV has almost disappeared and the peak at 400.6 eV is dominant. Similar C 1s XPS spectra (see Figure S4a) only show a pronounced shift at the transition from multilayers to the monolayer. The ratio between the N 1s and C 1s intensity is plotted in Figure 2b, showing a pronounced drop by a factor of ~1/3 following the last annealing to 423 K. The absolute C 1s and N 1s intensities (see Figure S4b) are reduced following the annealing steps, which is attributed to desorption. Only the nitrogen signal is reduced after the last annealing to 423 K.

The N 1s peaks at high binding energies (between 399.8 and 400.6 eV) are attributed to mono-, di-, and trioctylamine in accordance with previous assignments.[8] The peaks with a lower binding energy (398.9 and 399.2 eV) are proposed to stem from partly dehydrogenated amines formed in the initial annealing steps. The strong decrease in the N/C ratio following annealing to 423 K is consistent with formation of di- and trioctylamine along with desorption of lighter nitrogen-containing products.

In subsequent experiments, trioctylamine was deposited onto the Au(111) surface at room temperature (~300 K) and imaged by STM. As shown in Figure 1f,g, a honeycomb structure is formed which is identical to that observed for octylamine after annealing above 400 K. The trioctyl honeycomb structure is still found after annealing to 400 K and could also only be imaged at positive bias. Since, in general, self-assembled molecular structures are very sensitive to even slight perturbations to the molecular building blocks, the observation of identical honeycomb structures confirms that trioctylamine is formed by thermal reaction of octylamine. The coexisting zigzag structure is accordingly attributed to dioctylamine but could also involve other species formed after deprotonation such as, for example, dioctyl hydrazine. Other byproducts may be contained in disordered areas observed by STM (see Figure S3a).

In summary, the combined STM and XPS data show that, upon annealing to ~400 K, octylamine undergoes dehydrogenation of the amino group followed by formation of trioctylamine. A substitution reaction between amines is not anticipated to happen spontaneously in conventional solution phase chemistry, and we therefore propose that the Au(111) surface surprisingly acts as a catalyst for the reaction in vacuum. The energy barrier toward direct dissociation of C−N bonds on the Au(111) surface has been calculated to 3.5 eV using density functional theory,[19] suggesting that this process is not anticipated to occur at the investigated temperatures. We speculate that the barrier toward C−N bond dissociation is lowered by bond formation to other amino groups in the close-packed overlayer during reaction.

Acknowledgment. We acknowledge funding from the EU programs MONET and PICO-INSIDE, and the Danish Natural Science Research Council through funding for the iNANO center. We thank K.V. Gothelf for helpful discussions.

Supporting Information Available: Additional figures. This material is available free of charge via the Internet at http://pubs.acs.org.

References

(1) Davies, P. R.; Keel, J. M. *Surf. Sci.* **2000**, *469*, 204–213.
(2) Yao, Y. F. Y. *J. Phys. Chem.* **1964**, *68*, 101–105.
(3) Davies, P. R.; Keel, J. M. *Catal. Lett.* **1999**, *58*, 99–102.
(4) Maseri, F.; Peremans, A.; Darville, J.; Gilles, J. M. *J. Electron Spectrosc. Relat. Phenom.* **1990**, *54–55*, 1059–1064.
(5) Chorkendorff, I.; Russell, J. N.; Yates, J. T. *J. Chem. Phys.* **1987**, *86*, 4692–4700.
(6) Thomas, P. A.; Masel, R. I. *J. Vac. Sci. Technol. A* **1987**, *5*, 1106–1108.
(7) Hwang, S. Y.; Seebauer, E. G.; Schmidt, L. D. *Surf. Sci.* **1987**, *188*, 219–234.
(8) Chen, J. J.; Winograd, N. *Surf. Sci.* **1995**, *326*, 285–300.
(9) Baca, A. G.; Schulz, M. A.; Shirley, D. A. *J. Chem. Phys.* **1985**, *83*, 6001–6008.
(10) Xu, C.; Sun, Li.; Kepley, L. J.; Crooks, R. M. *Anal. Chem.* **1993**, *65*, 2102–2107.
(11) Kang, D. H.; Chatterjee, B.; Herceg, E.; Trenary, M. *Surf. Sci.* **2003**, *540*, 23–38.
(12) Cao, X.; Hamers, R. J. *Surf. Sci.* **2003**, *523*, 241–251.
(13) Eves, B. J.; Fan, C.; Lopinski, G. P. *Small* **2006**, *2*, 1379–84.
(14) Claypool, C. L.; Faglioni, F.; Goddard, W. A.; Gray, H. B.; Lewis, N. S.; Marcus, R. A. *J. Phys. Chem. B* **1997**, *101*, 5978–5995.
(15) Weigelt, S.; Busse, C.; Bombis, C.; Knudsen, M. M.; Gothelf, K. V.; Strunskus, T.; Wöll, C.; Dahlbom, M.; Hammer, B.; Lægsgaard, E.; Besenbacher, F.; Linderoth, T. R. *Angew. Chem., Int. Ed.* **2007**, *46*, 9227–9230.
(16) Lægsgaard, E.; Besenbacher, F.; Mortensen, K.; Stensgaard, I. *J. Microsc.* **1988**, *152*, 663–669.
(17) Nyholm, R.; Andersen, J. N.; Johansson, U.; Jensen, B. N.; Lindau, I. *Nucl. Instrum. Methods A* **2001**, *467*, 520–524.
(18) Wetterer, S. M.; Lavrich, D. J.; Cummings, T.; Bernasek, S. L.; Scoles, G. *J. Phys. Chem. B* **1998**, *102*, 9266–9275.
(19) Li, J.; Li, R. F.; Wang, G. C. *J. Phys. Chem. B* **2006**, *110*, 14300–14303.

JA710227G